

# Reversible Iodine Capture by Non-Porous Pillar[6]arene Crystals

Kecheng Jie, Yujuan Zhou, Errui Li, Zhengtao Li, Run Zhao and Feihe Huang\*

*State Key Laboratory of Chemical Engineering, Center for Chemistry of High-Performance & Novel Materials, Department of Chemistry, Zhejiang University, Hangzhou, Zhejiang 310027, P. R. China; Fax and Tel: +86-571-8795-3189; Email : [fhuang@zju.edu.cn](mailto:fhuang@zju.edu.cn)*

## Supporting Information (28 pages)

1. <i>Materials</i>	S2
2. <i>Methods</i>	S2
3. <i>Crystallography Data</i>	S5
4. <i>Characterization of Activated <b>EtP5</b> Crystals (<b>EtP5</b> <math>\alpha</math>), <b>EtP6</b> Crystals (<b>EtP6</b> <math>\beta</math>) and <b>EtP7</b> Crystals (<b>EtP7</b> <math>\alpha</math>)</i>	S6
5. <i>Porosity Measurements</i>	S10
6. <i>Iodine Vapor Uptake Experiments</i>	S12
7. <i>Iodine Capture Experiments in Solution</i>	S17
8. <i>Iodine Release</i>	S19
9. <i>Iodine Release from Single Crystals of <b>I</b><sub>2</sub>@<b>EtP6</b> in Cyclohexane and Single-Crystal to Single-Crystal Transformation</i>	S21
10. <i>Recyclability of <b>EtP6</b> in Iodine Capture</i>	S24
11. <i>References</i>	S28

## 1. Materials

*p*-Diethoxybenzene was purchased from JKchemicals and used as received. All other chemicals including iodine were purchased from Sigma-Aldrich and used as received. **EtP5**, **EtP6** and **EtP7** were synthesized as described previously.<sup>1</sup> Activated crystalline **EtP5** (**EtP5 $\alpha$** ) was recrystallized from tetrahydrofuran first and dried under vacuum at 60 °C overnight. Activated crystalline **EtP6** (**EtP6 $\beta$** ) was recrystallized from acetone first and dried under vacuum at 140 °C overnight. Activated crystalline **EtP7** (**EtP7 $\alpha$** ) was obtained as synthesized and dried under vacuum at 60 °C overnight.

## 2. Methods

**2.1. Thermogravimetric Analysis.** Thermogravimetric Analysis (TGA) was carried out using a Q5000IR analyzer (TA instruments) with an automated vertical overhead thermobalance. The samples were heated at the rate of 10 °C/min using N<sub>2</sub> as the protective gas.

**2.2. Solution NMR.** Solution <sup>1</sup>H NMR spectra were recorded at 400.13 MHz using a Bruker Avance 400 NMR spectrometer.

**2.3. Powder X-Ray Diffraction.** Powder X-ray diffraction (PXRD) data were collected on a Rigaku Ultimate-IV X-ray diffractometer operating at 40 kV/30 mA using the Cu K $\alpha$  line ( $\lambda = 1.5418 \text{ \AA}$ ). Data were measured over the range 5–40 ° in 5 °/min steps over 7 min.

**2.4. UV-Vis Spectra.** UV-vis spectra were taken on a PerkinElmer Lambda 35 UV-vis spectrophotometer.

**2.5. Gas Adsorption Analysis.** Low-pressure gas adsorption measurements were performed on a Micromeritics Accelerated Surface Area and Porosimetry System (ASAP) 2020 surface area analyzer. Samples were degassed under dynamic vacuum

for 12 h at 60 °C prior to each measurement. N<sub>2</sub> isotherms were measured using a liquid nitrogen bath (77 K).

**2.6. Optical Microscopy and Optical Images.** Optical microscopy white-light images were recorded by an AmScope SM-1TSW2 stereomicroscope. Optical images were taken by a Cannon 60D camera.

**2.7. The Fourier Transform Infrared (FT-IR) Spectroscopy.** The FT-IR spectra were recorded from KBr pellets containing ca. 1 mg of the compound in the range 4000-400 cm<sup>-1</sup> on a Perkin–Elmer one FT-IR spectrophotometer.

**2.8. Scanning Electron Microscopy and Energy-Dispersive Spectroscopy.** Scanning electron microscopy investigations were carried out on a HITACHI SU-8010 instrument at an electron acceleration voltage of 15 kV.

**2.9. Single Crystal Growth.** Single crystals of I<sub>2</sub>@**EtP6** were obtained as follows: 2 mg of **EtP6** powder was put in small vials where 2 mL of a 1-chlorobutane solution of iodine (10 mg/mL) were added. The resultant purple solution was allowed to free stand to give red crystals in 1 day. Single crystals of Cy@**EtP6** were obtained as follows: 2 mg of **EtP6** powder was dissolved in 2 mL of ethylbenzene in an open 5 mL vial, which was placed in a sealed 20 mL vial containing 3 mL of cyclohexane. Colorless single crystals were obtained overnight.

#### **2.10. Single Crystal X-ray Diffraction**

Single crystal X-ray data sets were measured on a Rigaku MicroMax-007 HF rotating anode diffractometer (Mo-K $\alpha$  radiation,  $\lambda = 0.71073$  Å, Kappa 4-circle goniometer, Rigaku Saturn 724+ detector). Unless stated solvated single crystals, isolated from the crystallization solvent, were immersed in a protective oil, mounted on a MiTeGen loop, and flash cooled under a dry nitrogen gas flow. Empirical absorption corrections,

using the multi-scan method, were performed with the program SADABS.<sup>3,4</sup> Structures were solved with SHELXD<sup>5</sup> or SHELXT,<sup>6</sup> or by direct methods using SHELXS,<sup>7</sup> refined by full-matrix least squares on  $|F|^2$  by SHELXL,<sup>8</sup> and interfaced through the programme OLEX2.<sup>9</sup> Unless stated all non-H-atoms were refined anisotropically, and H-atoms were fixed in geometrically estimated positions and refined using the riding model. Supplementary CIFs, which include structure factors, are available free of charge from the Cambridge Crystallographic Data Centre (CCDC) via [www.ccdc.cam.ac.uk/data\\_request/cif](http://www.ccdc.cam.ac.uk/data_request/cif).

### 3. Crystallography Data

**Table S1.** Experimental single crystal X-ray data for **EtP6** structures.

Formula	<b>EtP6</b> ·I <sub>2</sub>	<b>EtP6</b>
Crystallization Solvent	1-chlorobutane	Cyclohexane/ethylbenzene
Collection	173 K	293 K
Temperature		
Formula	C <sub>66</sub> H <sub>84</sub> I <sub>2</sub> O <sub>12</sub>	C <sub>66</sub> H <sub>84</sub> O <sub>12</sub>
<i>Mr</i>	1323.13	1069.33
Crystal Size [mm]		
Crystal System	Triclinic	Orthorhombic
Space Group	<b>P</b> $\bar{1}$	<i>Fd</i>
<i>a</i> [Å]	10.4135(5)	12.6104(7)
<i>b</i> [Å]	13.1885(6)	26.6968(13)
<i>c</i> [Å]	13.7554(7)	45.345(2)
$\alpha$ [°]	106.470(2)	
$\beta$ [°]	103.657(2)	
$\gamma$ [°]	110.715(2)	
<i>V</i> [Å <sup>3</sup> ]	1570.83 (13)	15265.7(13)
<i>Z</i>	1	8
<i>D</i> <sub>calcd</sub> [g cm <sup>-3</sup> ]	1.399	0.931
$\mu$ [mm <sup>-1</sup> ]	8.342	0.063
F(000)	682	4608
2 $\theta$ range [°]	7.23 – 133.26	5.66 – 59.01
Reflections collected	16006	23927
Independent reflections, <i>R</i> <sub>int</sub>	5496, 0.0261	3620, 0.0217
Obs. Data [ <i>I</i> > 2 $\sigma$ ( <i>I</i> )]	5164	2237
Data / restraints / parameters	5496 / 0 / 367	3620 / 0 / 180
Final <i>R</i> <sub>1</sub> values ( <i>I</i> > 2 $\sigma$ ( <i>I</i> ))	0.0320	0.0730
Final <i>R</i> <sub>1</sub> values (all data)	0.0346	0.1033
Final <i>wR</i> ( <i>F</i> <sub>2</sub> ) values (all data)	0.0779	0.2544
Goodness-of-fit on <i>F</i> <sup>2</sup>	1.070	1.038
Largest difference peak and hole [e.Å <sup>-3</sup> ]	0.970 / -1.198	0.201 / -0.178
CCDC	1570931	1570932

#### 4. Characterization of Activated EtP5 Crystals (EtP5 $\alpha$ ), EtP6 Crystals (EtP6 $\beta$ ) and EtP7 Crystals (EtP7 $\alpha$ )

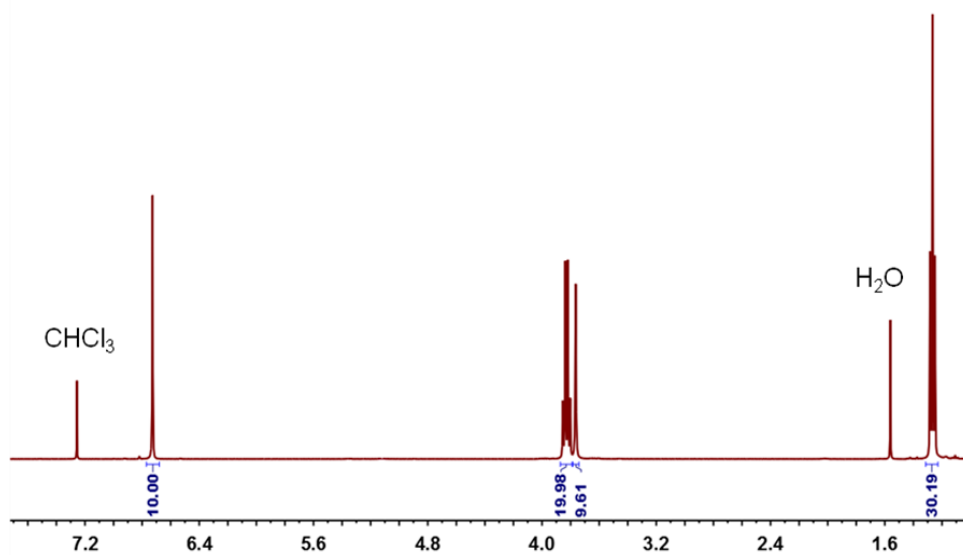


**Figure S1.** <sup>1</sup>H NMR spectrum (400 MHz, CDCl<sub>3</sub>, 293 K) of **EtP5 $\alpha$** .

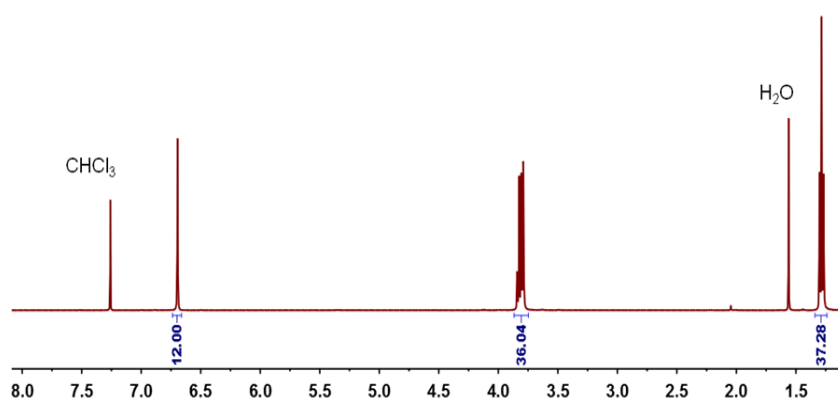


**Figure S2.** <sup>1</sup>H NMR spectrum (400 MHz, CDCl<sub>3</sub>, 293 K) of **EtP6 $\beta$** .

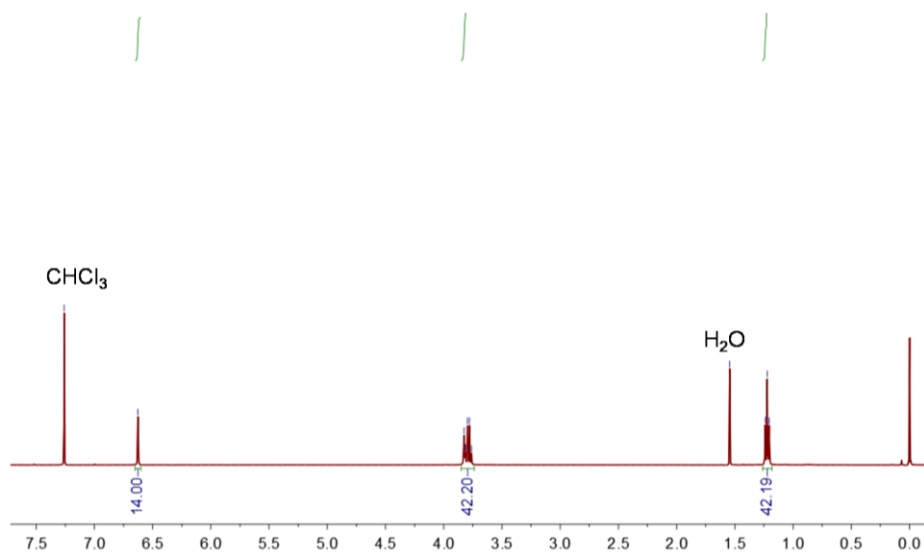


**Figure S3.**  $^1\text{H}$  NMR spectrum (400 MHz,  $\text{CDCl}_3$ , 293 K) of **EtP7 $\alpha$** .

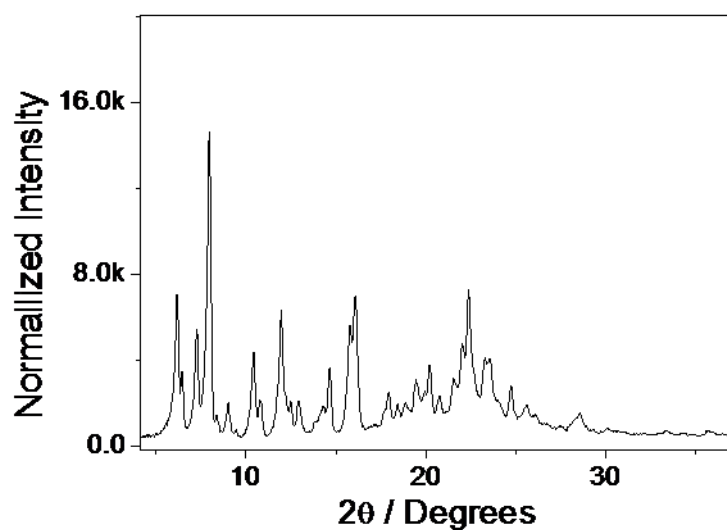


**Figure S4.** Powder X-ray diffraction pattern of **EtP5 $\alpha$** .

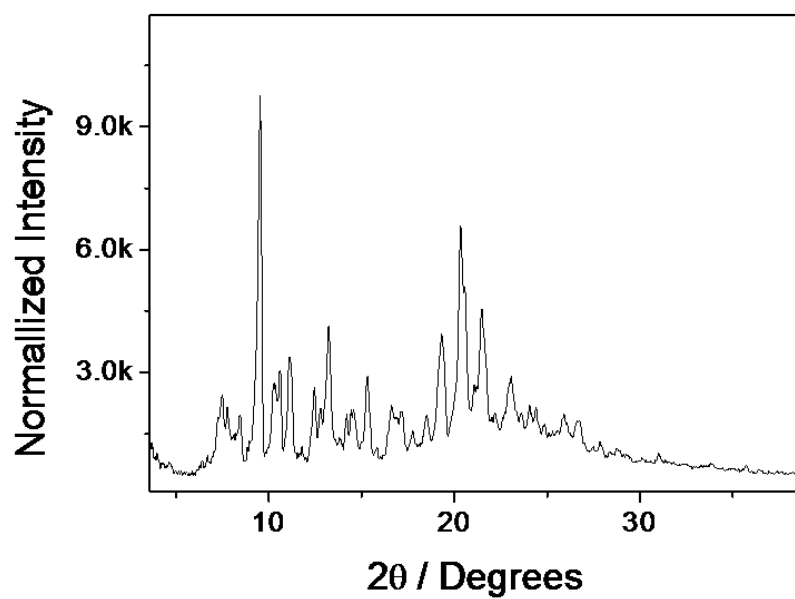


**Figure S5.** Powder X-ray diffraction pattern of **EtP6β**.

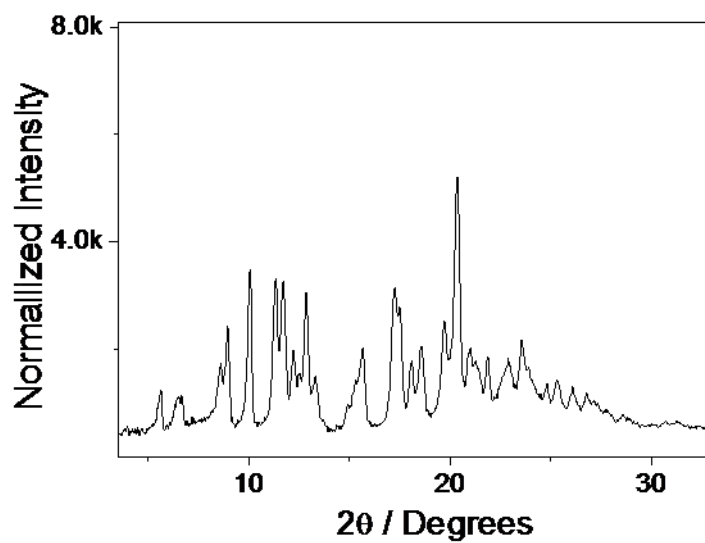


**Figure S6.** Powder X-ray diffraction pattern of **EtP7α**.

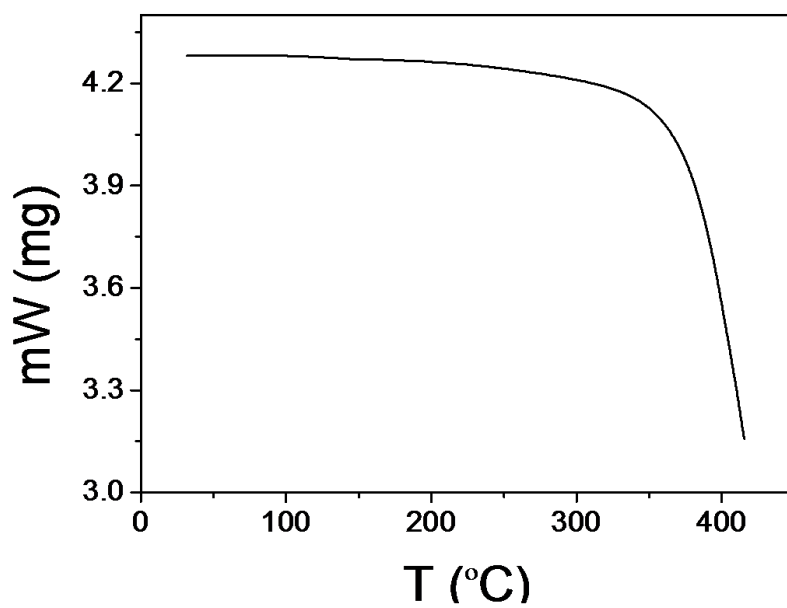


**Figure S7.** Thermogravimetric analysis of desolvated **EtP5**.

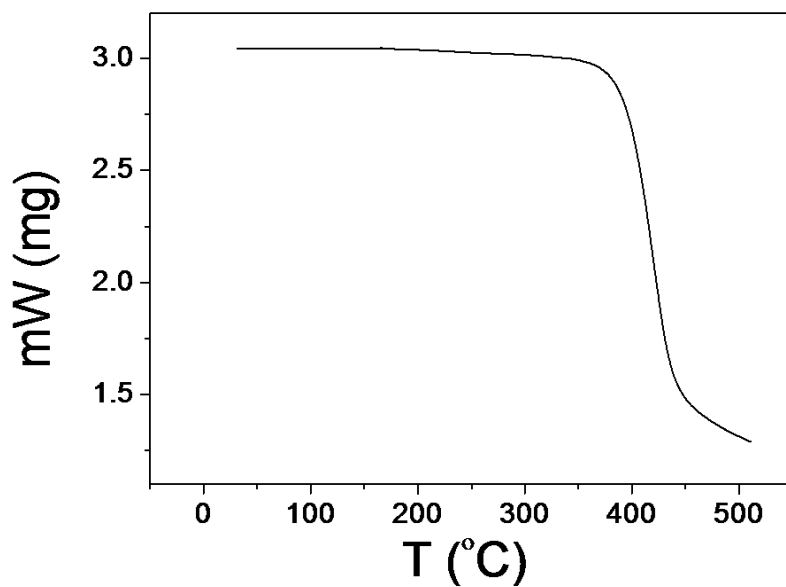


**Figure S8.** Thermogravimetric analysis of desolvated **EtP6**.

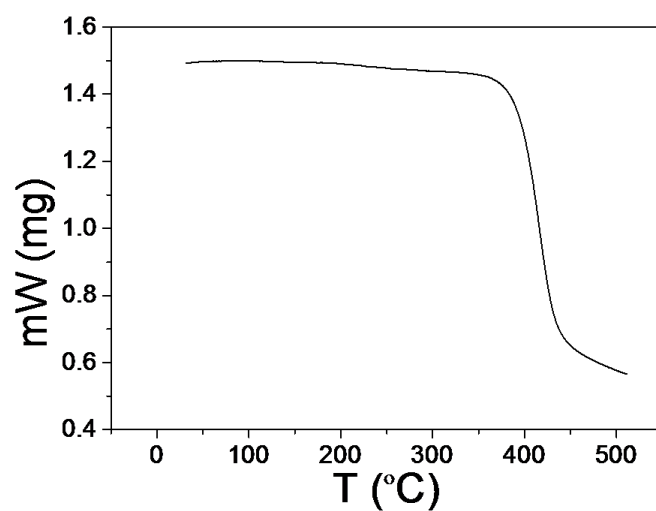


**Figure S9.** Thermogravimetric analysis of desolvated **EtP7**.

## 5. Porosity Measurements

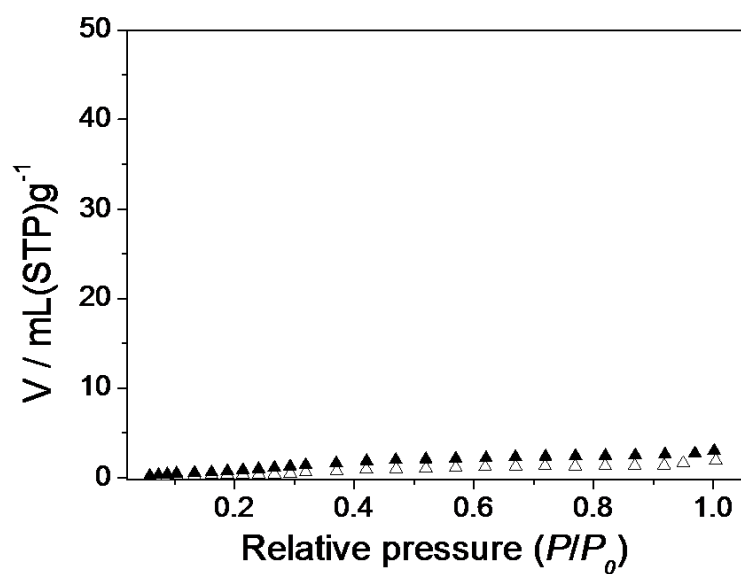


**Figure S10.** N<sub>2</sub> adsorption isotherm of **EtP5 $\alpha$** . Adsorption, closed symbols; desorption, open symbols.

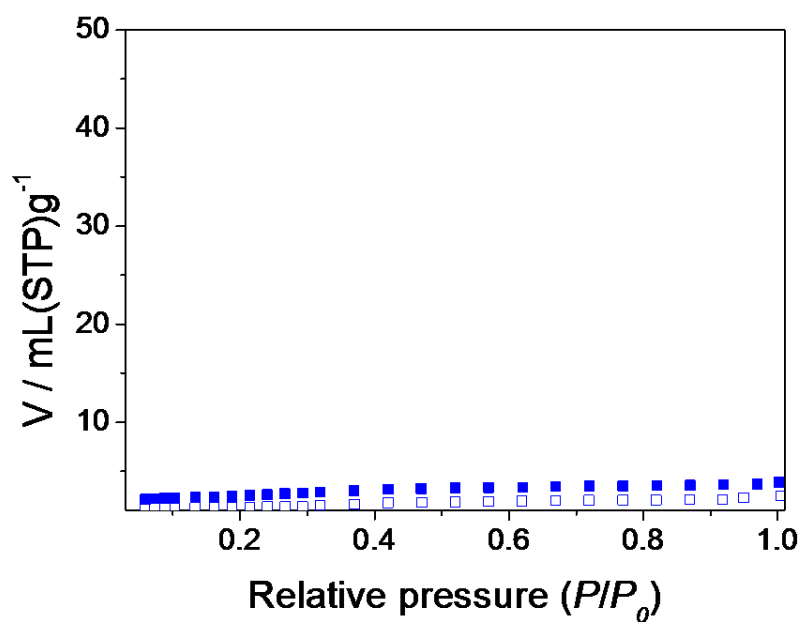


**Figure S11.** N<sub>2</sub> adsorption isotherm of **EtP6β**. Adsorption, closed symbols; desorption, open symbols.

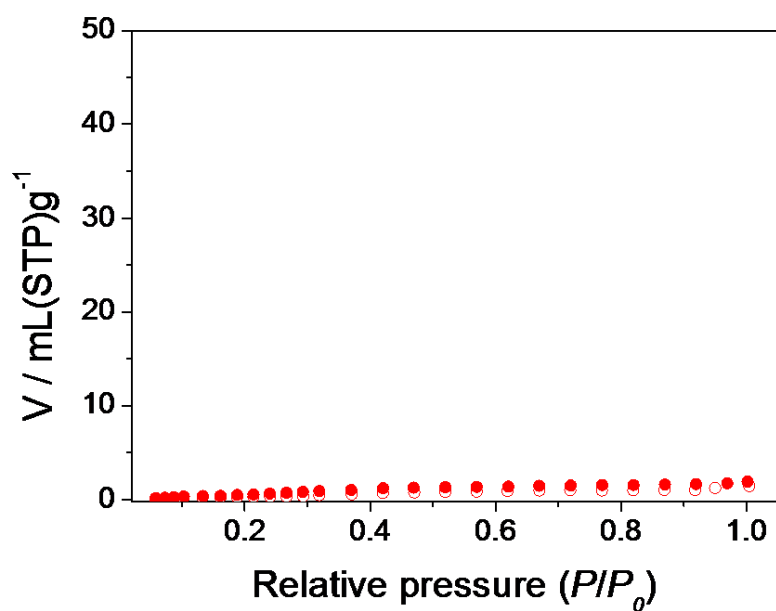


**Figure S12.** N<sub>2</sub> adsorption isotherm of **EtP7α**. Adsorption, closed symbols; desorption, open symbols.

## 6. Iodine Vapor Uptake Experiments

Time-dependent iodine vapor uptake experiments were performed in the following procedure: 10 mg of activated pillararene crystals in an open thermoresistant plastic cap (0.5 mL) and 500 mg of iodine was placed in a sealed glass vial (7 mL) and heated at 358.15 K and 1.0 bar using an oil bath. Note that both the iodine and caps were placed below the top level of the oil bath. This avoids temperature gradient, which may cause iodine deposition on the surface of pillararene powder. After adsorption of the iodine vapor (0–2 h), the adsorbed pillararene powder was cooled down to room temperature and analyzed by TGA.

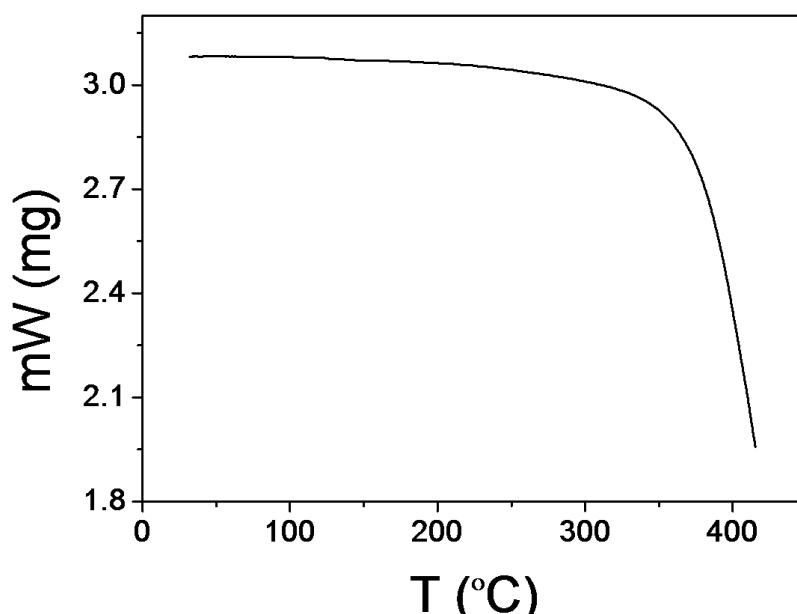


**Figure S13.** Thermogravimetric analysis of **EtP5 $\alpha$**  after adsorption of iodine vapor for 120 min.

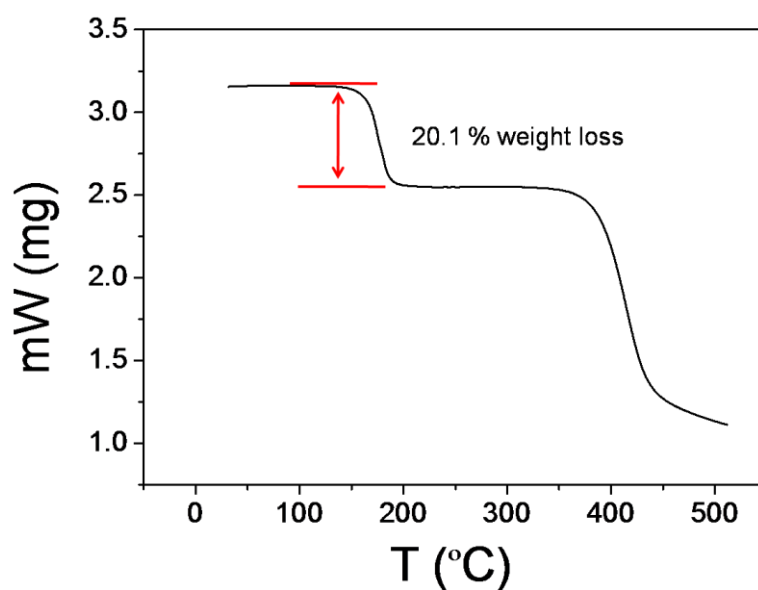


**Figure S14.** Thermogravimetric analysis of **EtP6 $\beta$**  after adsorption of iodine vapor for 120 min.

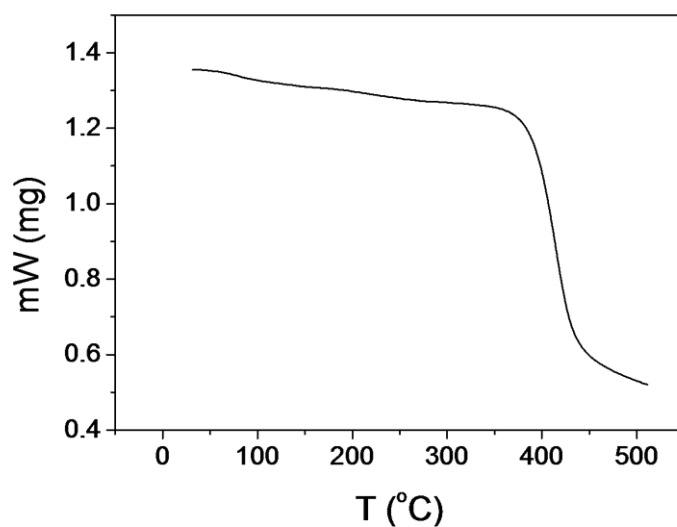


**Figure S15.** Thermogravimetric analysis of **EtP7 $\alpha$**  after adsorption of iodine vapor for 120 min.

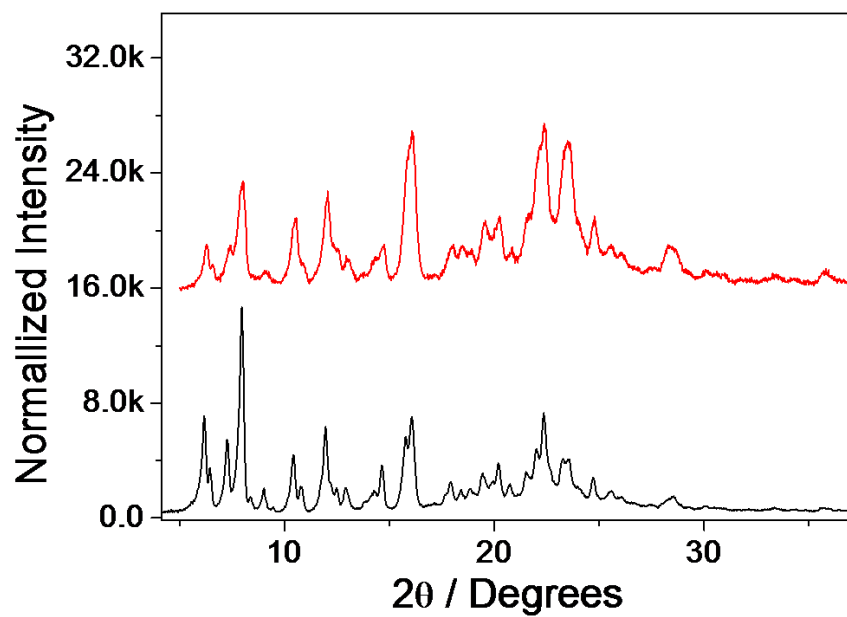


**Figure S16.** Powder X-ray diffraction patterns of **EtP5 $\alpha$**  (bottom) and **EtP5 $\alpha$**  after uptake of iodine vapor (Top).

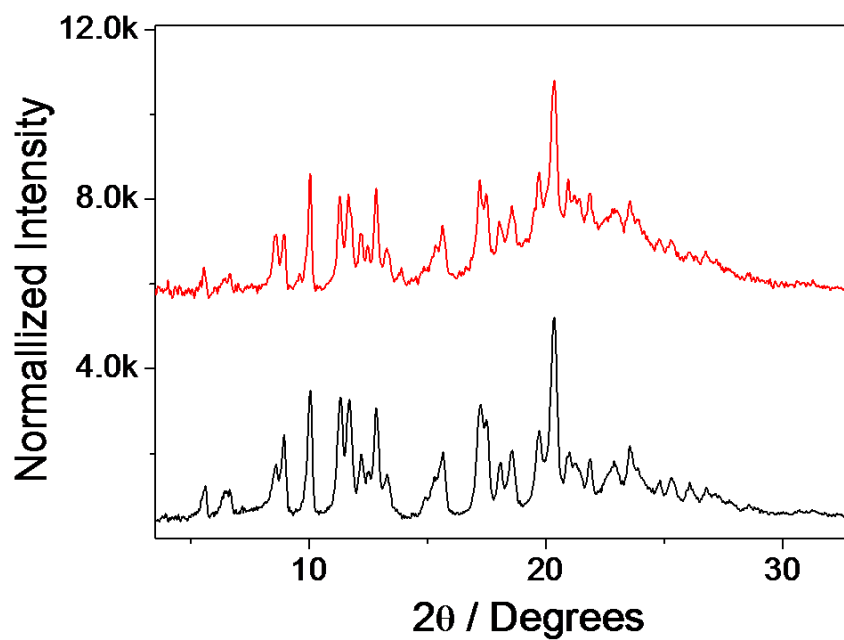


**Figure S17.** Powder X-ray diffraction patterns of **EtP7 $\alpha$**  (bottom) and **EtP7 $\alpha$**  after uptake of iodine vapor (Top).

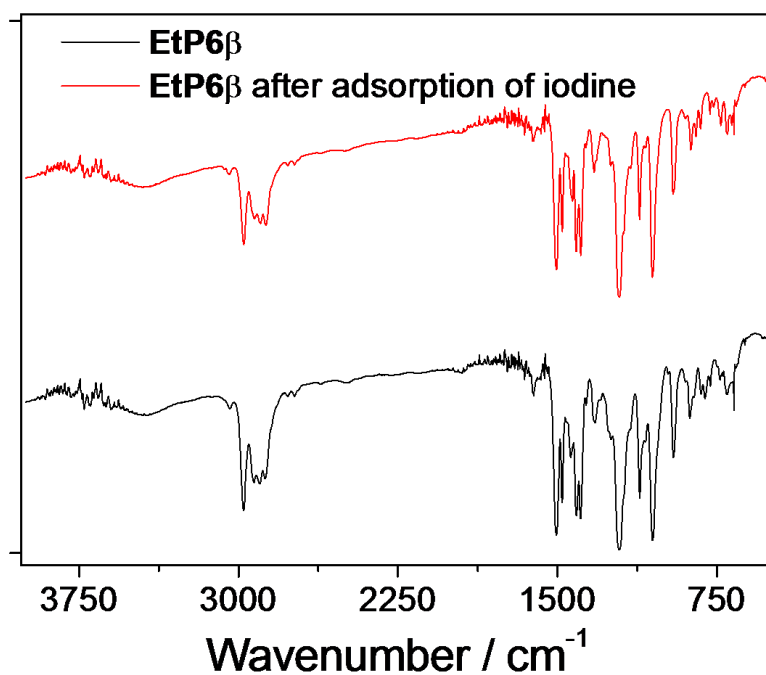


**Figure S18.** FT-IR spectra of **EtP6β** (bottom) and **EtP6β** after adsorption of iodine vapor for 120 min (Top).

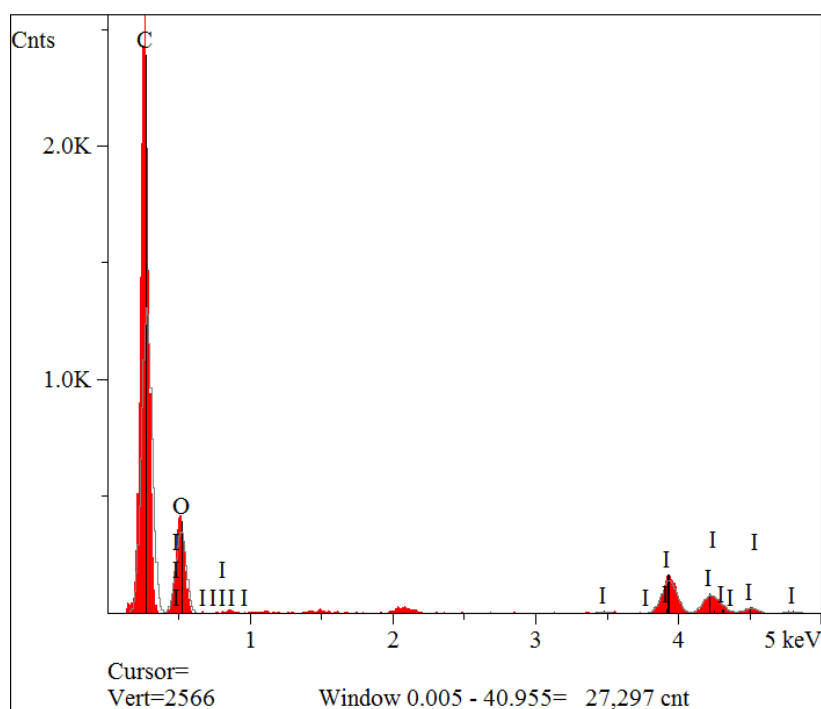


**Figure S19.** Energy-dispersive spectroscopy (EDS) analysis profile of **EtP6β** after adsorption of iodine.

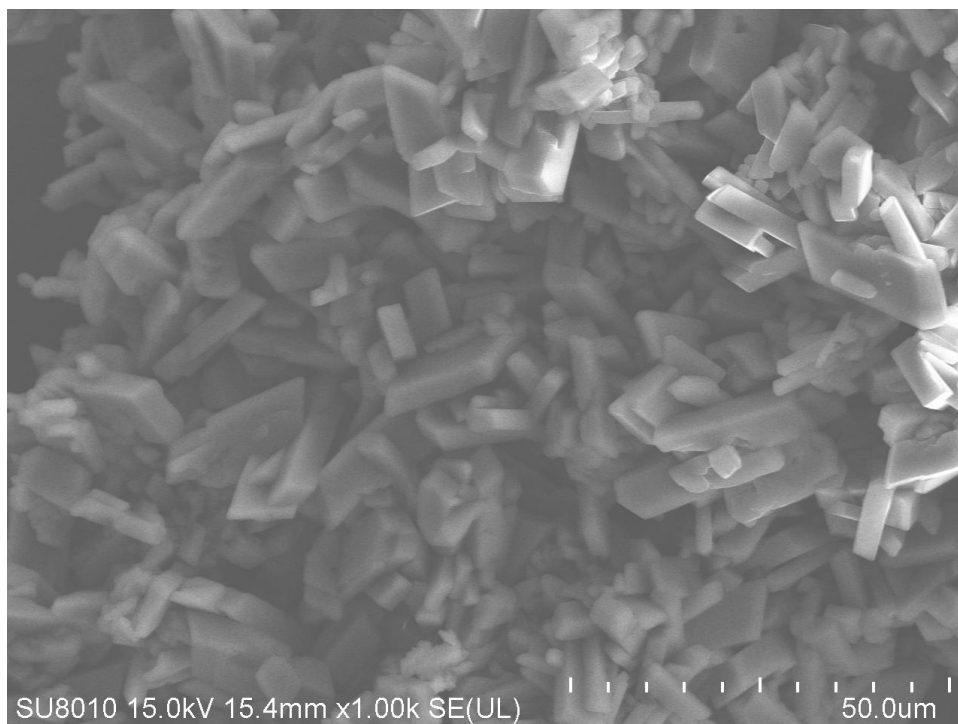


**Figure S20.** Scanning electron microscopy image of **EtP6 $\beta$**  crystalline solids after adsorption of iodine vapor.

## 7. Iodine Capture Experiments in Solution

In order to monitor the iodine capture of **EtP6** $\beta$  in solution, a time-dependent UV-Vis measurement was carried out. **EtP6** $\beta$  (3.0 mg) was added to an iodine solution (20.0 mM, 2 mL) with shaking. The UV-Vis spectrum of the solution was recorded over time.

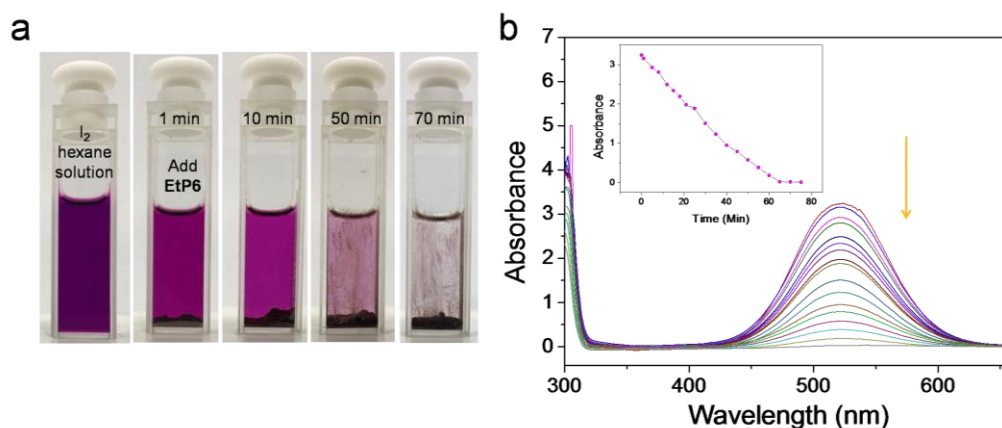


**Figure S21.** (a) Photographs showing a solution color change when 3 mg of **EtP6** $\beta$  crystalline solid was placed in an iodine/*n*-hexane solution. (b) Time-dependent UV/vis absorption spectra of the iodine/*n*-hexane solution upon addition of **EtP6** $\beta$  crystalline solid (3.0 mg). Inset: I<sub>2</sub> absorbance at 520 nm at various times.

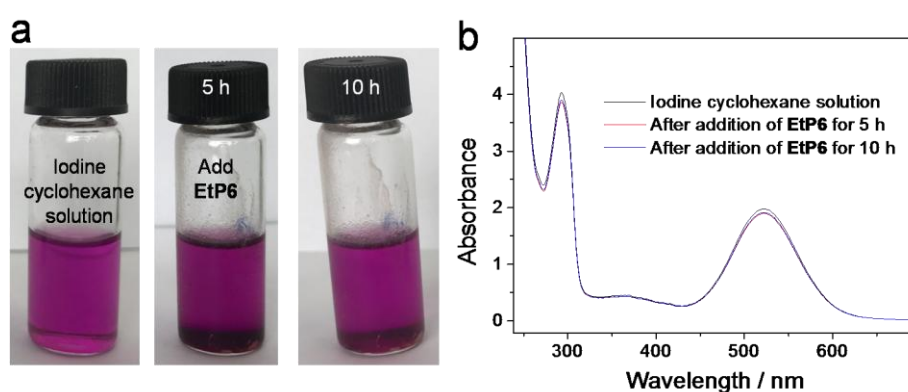


**Figure S22.** (a) Photographs of a solution when 3 mg of **EtP6** $\beta$  crystals were placed in an iodine/cyclohexane solution. (b) Time-dependent UV/vis absorption spectra of iodine/*n*-hexane solution upon addition of **EtP6** $\beta$  crystals (3.0 mg). Inset: I<sub>2</sub> absorbance at 520 nm at various times.

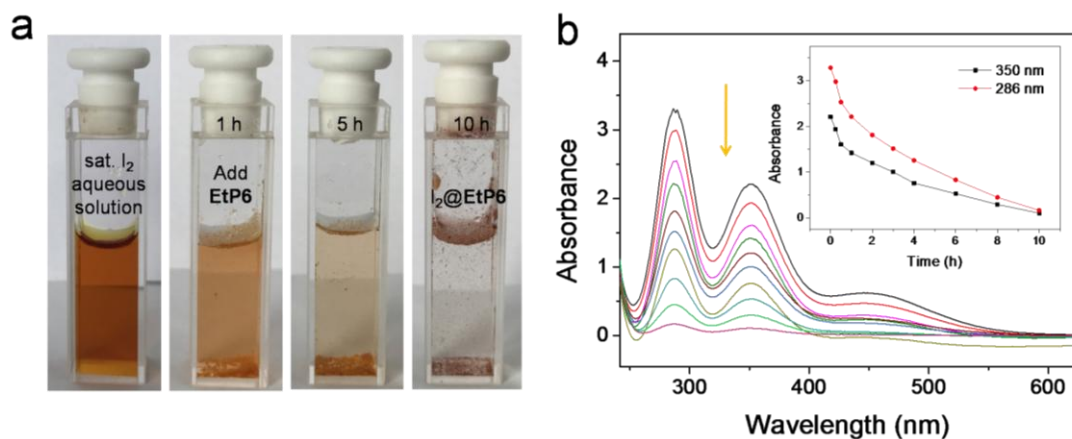


**Figure S23.** (a) Photographs of a saturated aqueous iodine solution at various times after 3 mg of **EtP6 $\beta$**  crystalline solid was placed into it. (b) Time-dependent UV/vis absorption spectra of the iodine aqueous solution upon addition of **EtP6 $\beta$**  crystalline solids (3.0 mg). Inset:  $I_2$  absorbance at 350 nm and 286 nm at various times, respectively.

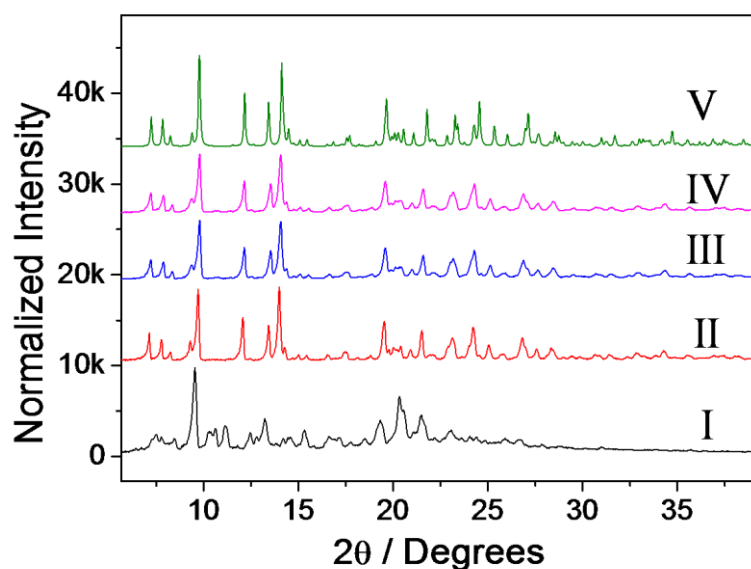


**Figure S24.** Powder X-ray diffraction (PXRD) patterns: (I) **EtP6 $\beta$** ; (II) **EtP6 $\beta$**  after adsorption of iodine vapor; (III) **EtP6 $\beta$**  after capture of iodine in *n*-hexane; (IV) **EtP6 $\beta$**  after capture of iodine in water; (V) simulated from single crystal structure of  $I_2@EtP6$ .

## 8. Iodine Release

In order to monitor the iodine release in a solvent, *in situ* a UV-Vis measurement was carried out. I<sub>2</sub>@EtP6 (3.0 mg) was added to a certain solvent (1.5 mL). The UV-Vis spectrum of the solution was recorded over time.

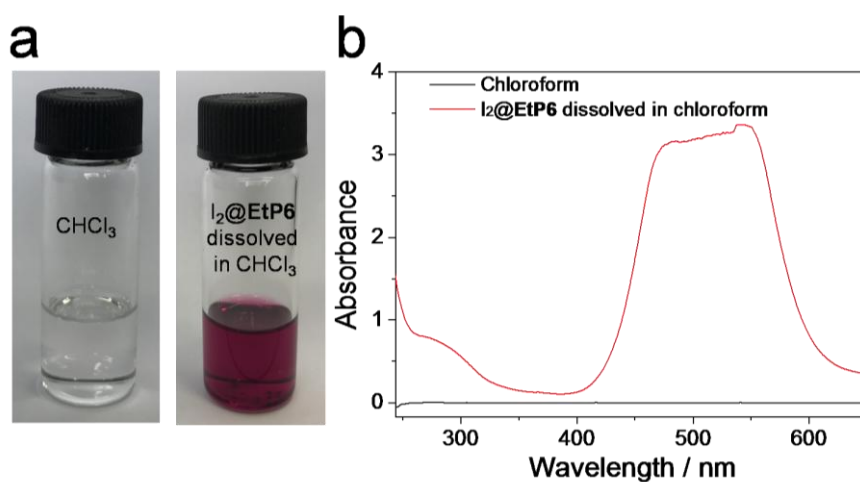


**Figure S25.** (a) Photographs of chloroform (left) and I<sub>2</sub>@EtP6 crystals dissolved in chloroform (right). (b) UV/vis absorption spectra of chloroform (black) and I<sub>2</sub>@EtP6 crystals dissolved in chloroform (red).

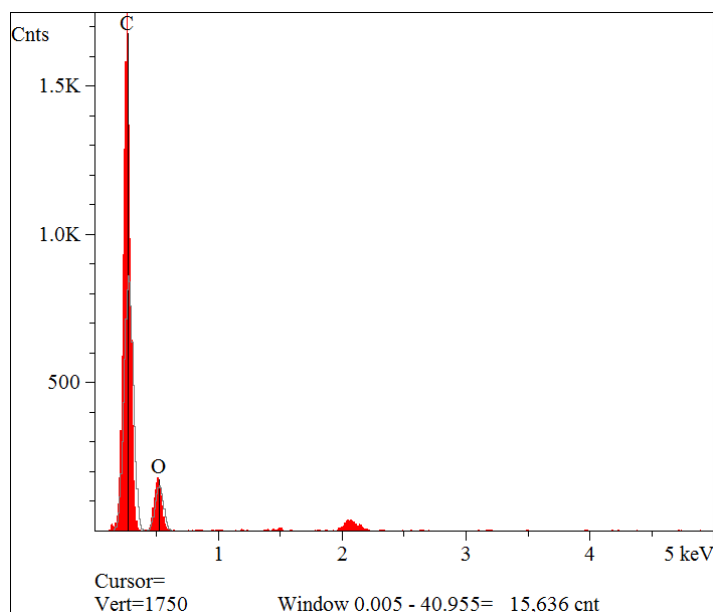


**Figure S26.** Energy-dispersive spectroscopy (EDS) analysis profile of I<sub>2</sub>@EtP6 after iodine release in cyclohexane.



**Figure S27.** Scanning electron microscopy image of  $I_2@EtP6$  crystalline solids after iodine release in cyclohexane.

## 9. Iodine Release from Single Crystals of $I_2@EtP6$ in Cyclohexane and Single-Crystal to Single-Crystal Transformation

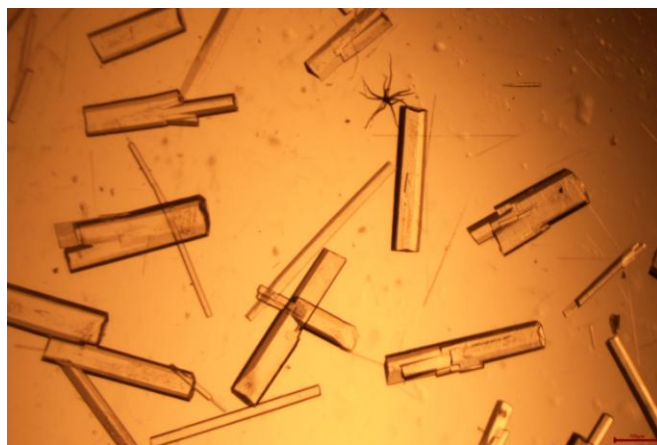


**Figure S28.** Microscopic images of **EtP6** single crystals obtained by cyclohexane diffusion into **EtP6**/ethylbenzene solution.

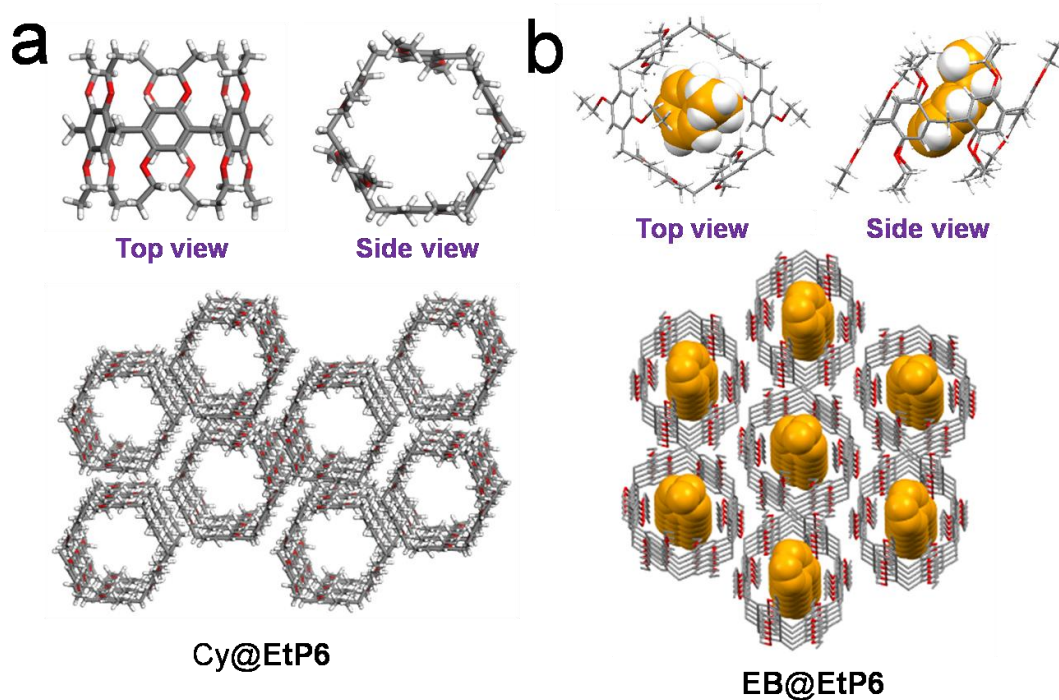


**Figure S29.** Single crystal structures: (a) **EtP6** obtained by cyclohexane diffusion into **EtP6** ethylbenzene solution; (b) ethylbenzene-loaded **EtP6** (**EB@EtP6**).<sup>12</sup> These two single crystal structures are different, indicating the solvate in (a) is cyclohexane (Cy). In the crystal structure of **Cy@EtP6**, cyclohexane is extremely disordered which can hardly be refined.

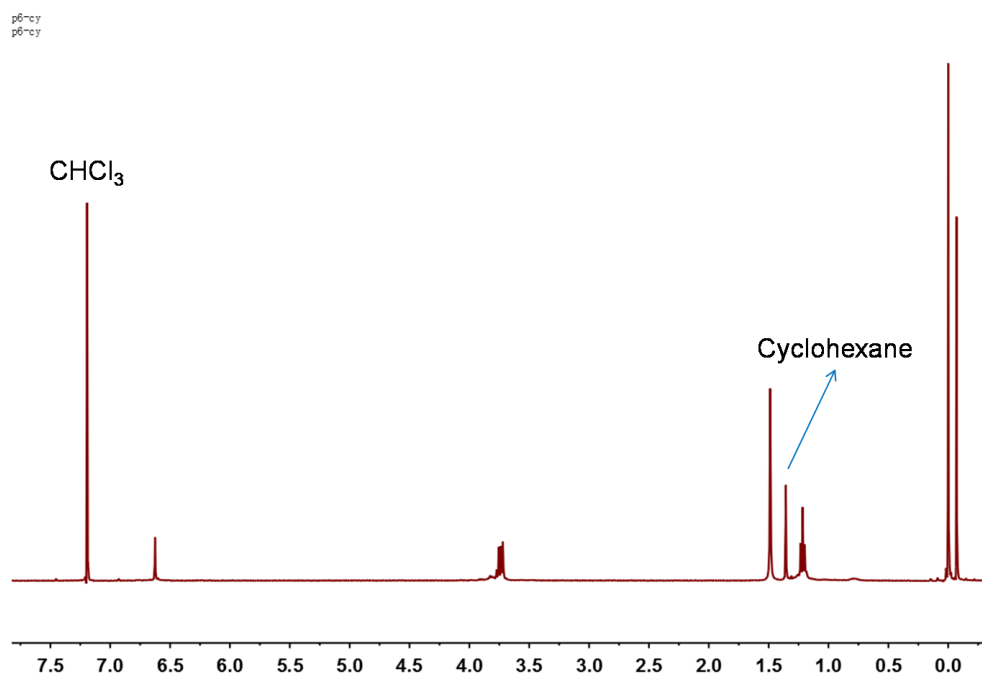


**Figure S30.**  $^1\text{H}$  NMR spectrum (400 MHz,  $\text{CDCl}_3$ , 293 K) of a  $\text{Cy@EtP6}$  single crystal. Only peaks related to cyclohexane and **EtP6** were found, indicating that the solvate molecules in the  $\text{Cy@EtP6}$  single crystal are actually cyclohexane.

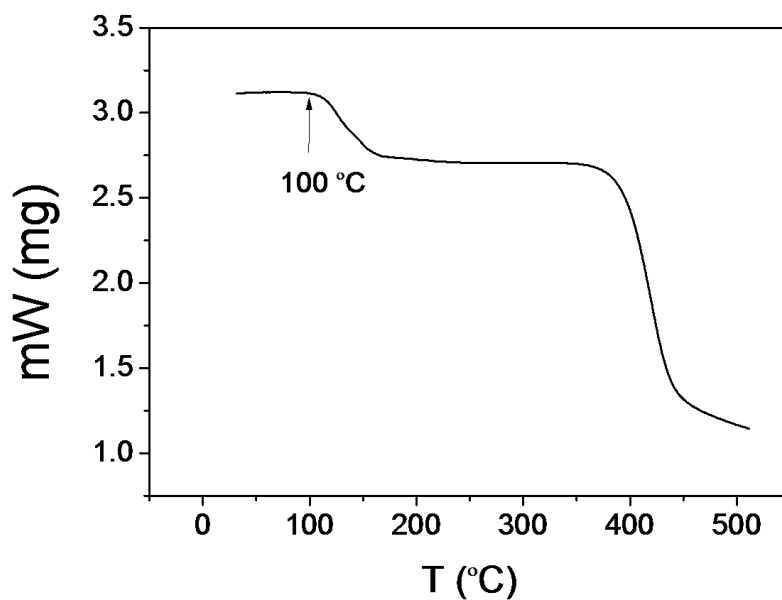


**Figure S31.** Thermogravimetric analysis of a  $\text{Cy@EtP6}$  single crystal.



**Figure S32.** Photographs showing the color change of cyclohexane (2 mL) upon addition of  $I_2@EtP6$  single crystals. The color change is due to the iodine release from  $I_2@EtP6$  single crystals.

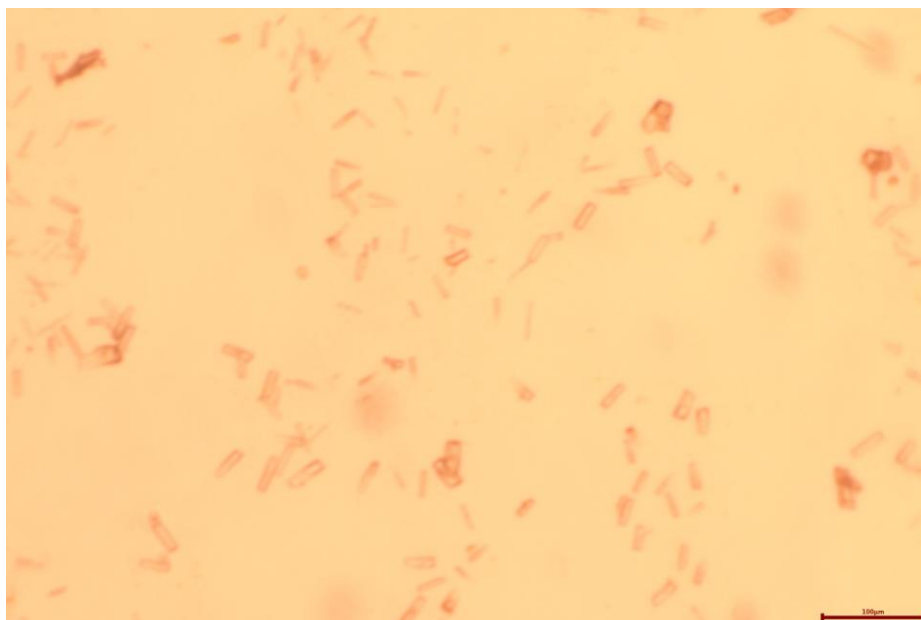


**Figure S33.** Microscopy images of **EtP6** single crystals obtained by immersing  $I_2@EtP6$  single crystals into cyclohexane for 2 days.

## 10. Recyclability of EtP6 in Iodine Capture

I<sub>2</sub>@ **EtP6** crystals were immersed in cyclohexane to release the adsorbed iodine. After complete release (no color change happened when the crystals were immersed in cyclohexane), the resultant crystals were desolvated under vacuum at 80 °C over 24 h and was determined to be **EtP6** $\beta$  by PXRD. The amorphous **EtP6** was prepared as follows: Pure **EtP6** was initially obtained through column chromatography. The solution was evaporated using rotary evaporator and the resultant solid was further desolvated at 100 °C under vacuum overnight. The obtained **EtP6** was determined to be amorphous by PXRD.

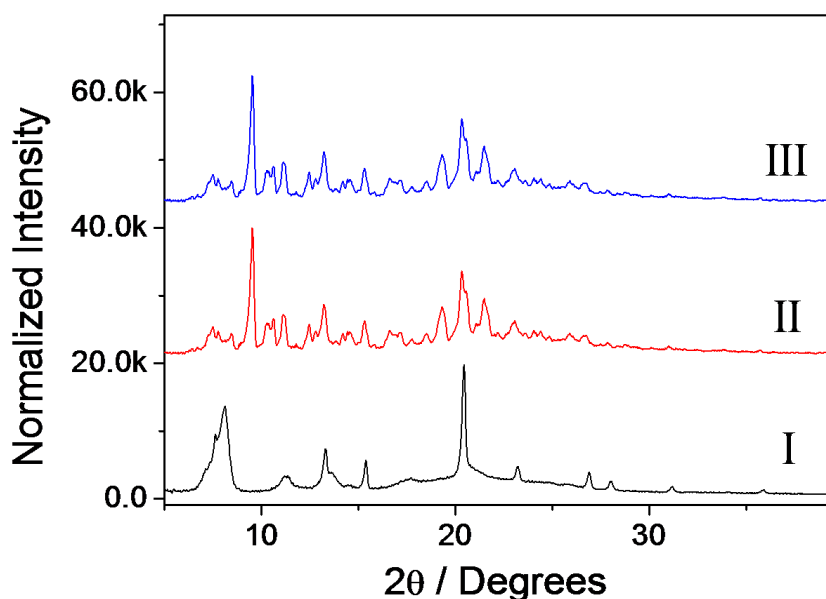


**Figure S34.** Powder X-ray diffraction (PXRD) patterns: (I) I<sub>2</sub>@**EtP6** after iodine release in cyclohexane (Cy@**EtP6**); (II) desolvated Cy@**EtP6**; (III) **EtP6** $\beta$ . Patterns (II) and (III) are almost the same, while pattern (I) is different, indicating the structural transformation from Cy@**EtP6** to **EtP6** $\beta$  upon desolvation.

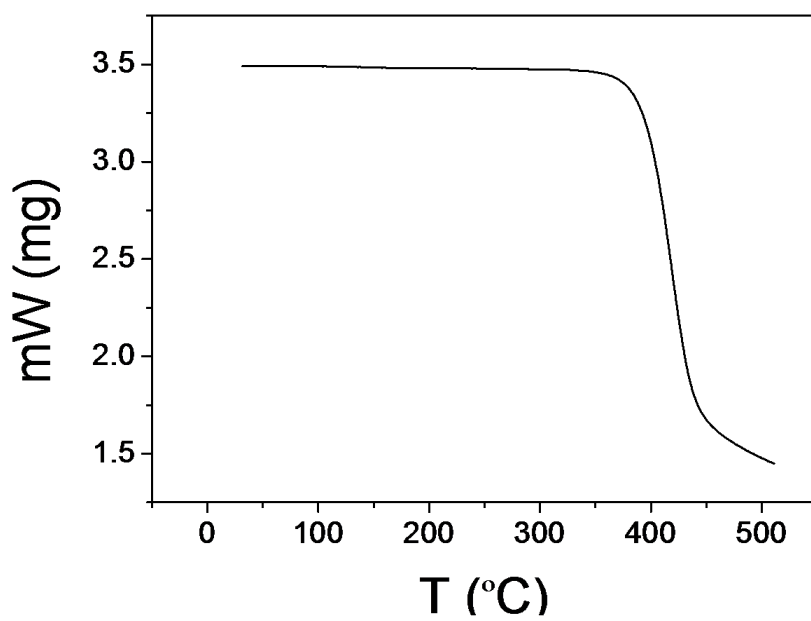


**Figure S35.** Thermogravimetric analysis of desolvated Cy@EtP6.

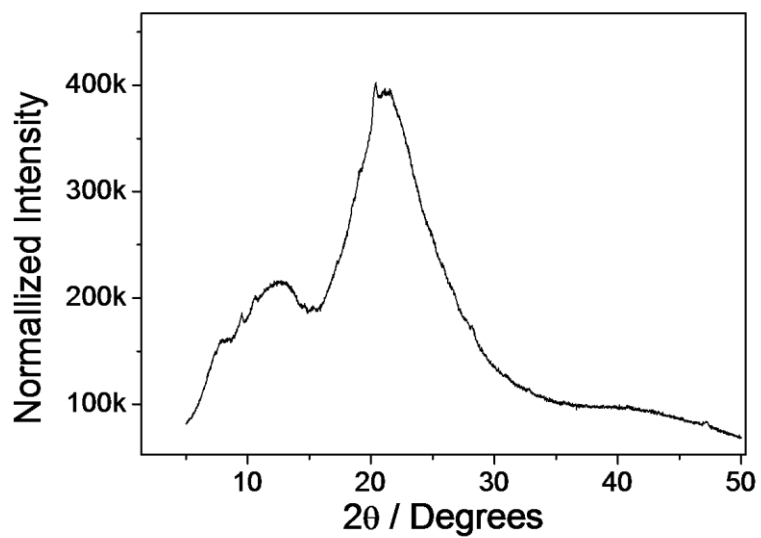


**Figure S36.** Powder X-ray diffraction pattern of amorphous EtP6.

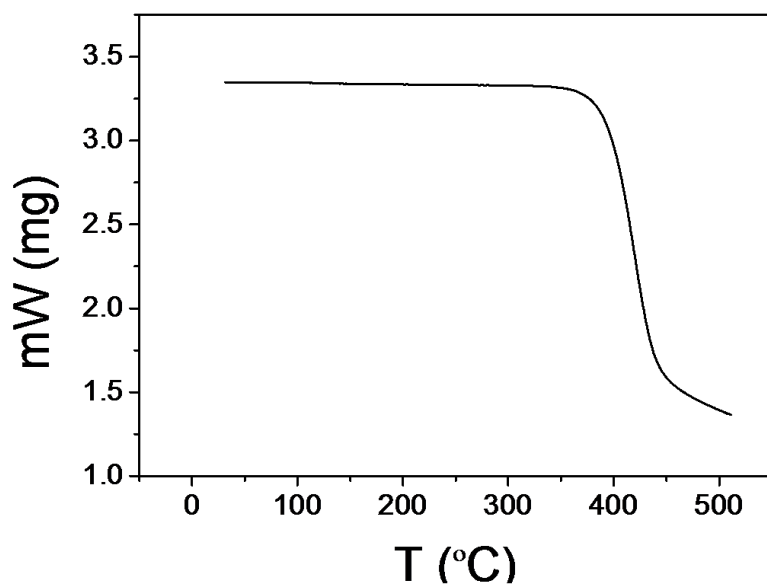


**Figure S37.** Thermogravimetric analysis of desolvated amorphous **EtP6**.

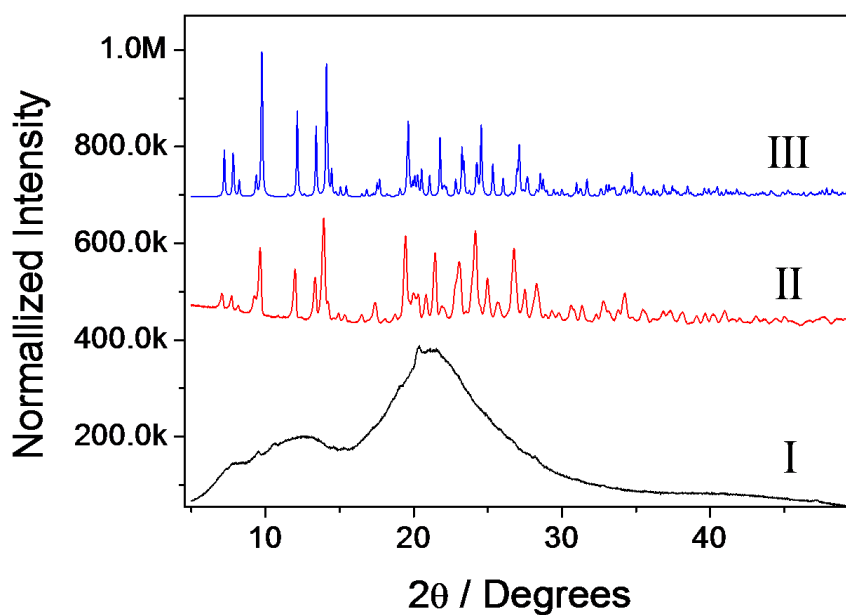


**Figure S38.** Powder X-ray diffraction patterns: (I) desolvated amorphous **EtP6**; (II) desolvated amorphous **EtP6** after adsorption of iodine vapor for 2 h at 358.15 K; (III) simulated from single crystal structure of  $I_2@EtP6$ .

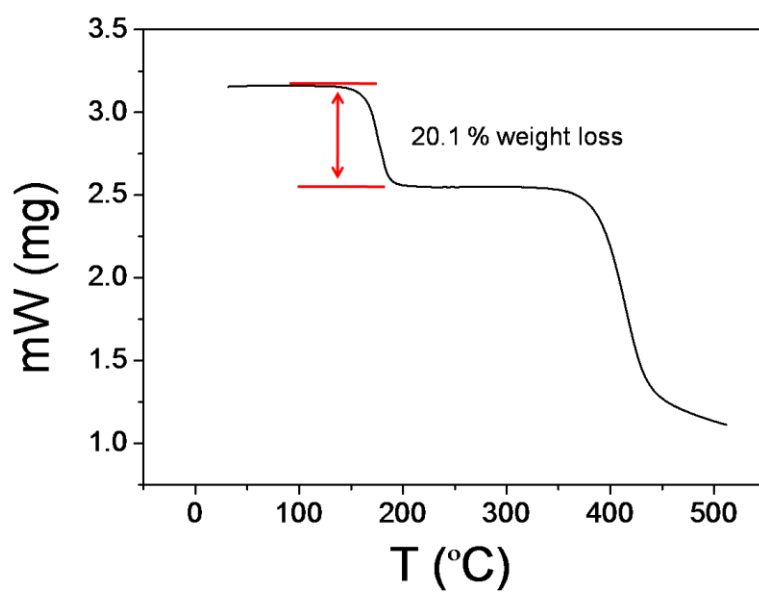


**Figure S39.** Thermogravimetric analysis of desolvated amorphous **EtP6** after adsorption of iodine vapor for 2 h at 358.15 K.

*References:*

- (1) Hu, X.-B.; Chen, Z.; Chen, L.; Zhang, L.; Hou, J.-L.; Li, Z.-T. *Chem. Commun.* **2012**, *48*, 10999.
- (2) Sheldrick, G. M. (*University of Göttingen, Germany*) **2008**.
- (3) Krause, L.; Herbst-Irmer, R.; Sheldrick, G. M.; Stalke, D. *J. Appl. Cryst.* **2015**, *48*, 3.
- (4) Sheldrick, G. *Acta Cryst. Sect. D* **2010**, *66*, 479.
- (5) Sheldrick, G. *Acta Cryst. Sect. A* **2015**, *71*, 3.
- (6) Sheldrick, G. M. *Acta Crystallogr., Sect. A: Found. Crystallogr.* **2008**, *64*, 112.
- (7) Sheldrick, G. *Acta Cryst. Sect. C* **2015**, *71*, 3.
- (8) Dolomanov, O. V.; Bourhis, L. J.; Gildea, R. J.; Howard, J. A. K.; Puschmann, H. *J. Appl. Cryst.* **2009**, *42*, 339.
- (9) Jie, K.; Liu, M.; Zhou, Y.; Little, M. A.; Bonakala, S.; Chong, S. Y.; Stephenson, A. Chen, L.; Huang, F.; Cooper, A. I. *J. Am. Chem. Soc.* **2017**, *139*, 2908.